

0.5 eV QCD Axion Cyclic Cosmology

NOAH BRAY-ALI¹

¹*Science Synergy*

ABSTRACT

A simple yet compelling physical picture is proposed for the nature of dark matter, dark energy, and the Big Bang. The proposal leads to a prediction with 4.4 parts per million precision for the 0.5 eV rest-mass energy of the quantum chromodynamic (QCD) axions that form the dark matter within this picture. A straightforward resolution of the Hubble tension follows from the agreement between the prediction for the present expansion rate of the universe within this picture and the best present determination from observations of the late universe.

Keywords: Cosmology (343) — Cosmological constant (334) — Dark energy (351) — Dark matter (353) — Baryon density (139) — Dark matter density (354) — Big Bang nucleosynthesis (151) — Horizontal branch stars (746) — Quasar absorption line spectroscopy (1317)

1. INTRODUCTION

In 2022 the Hubble tension between late-universe observations of the present expansion rate (A. G. Riess et al. 2022) and predictions within the standard cold dark matter cosmology with cosmological constant (Λ CDM) based on early-universe observations (Planck Collaboration et al. 2020; S. Aiola et al. 2020) reached the conventional 5.0σ threshold for the discovery of a new phenomenon in astrophysics. Several years before this conventional threshold was reached, astrophysicists were already stimulated by the accumulating evidence for the existence of a significant tension, and they began suggesting innovative alternative cosmologies that might reconcile early- and late-universe observations (V. Poulin et al. 2019). In 2024 the tension was confirmed on the late-universe side with James Webb Space Telescope (JWST) observations that rejected unrecognized crowding of Cepheid variable star photometry as an explanation of the Hubble tension at 8σ confidence (A. G. Riess et al. 2024a), and that validated the Hubble Space Telescope (HST) distance measurements on which the tension rests (A. G. Riess et al. 2024b).

On the early-universe side, the Dark Energy Spectroscopic Instrument (DESI) first-year observations of the peak in the galaxy-galaxy two-point correlation function

confirmed the Hubble tension in 2025, provided the results are interpreted within the standard Λ CDM cosmology (A. G. Adame et al. 2025). Similarly, in 2023 an independent combination of ground-based and space-based observations of the cosmic microwave background (CMB) power spectrum of angular fluctuations confirmed the tension, again within the framework of Λ CDM (L. Balkenhol et al. 2023). In 2024 the first comprehensive book-length review concluded that the Hubble tension remains an unsolved mystery (A. G. Riess 2024).

The purpose of this Letter is to propose a simple yet compelling physical picture for the nature of dark matter, dark energy, and the Big Bang. However, the picture offers a straightforward resolution of the Hubble tension, and this resolution is, therefore, the primary astrophysical motivation for considering the picture, despite the fact that, historically, the picture emerged from quite different motivations and considerations (See Section 2). In brief, the picture leads to the following high-precision prediction from first-principles for the value of the present expansion rate of universe (See Section 3 for details):

$$H_0 = 71.4 \text{ }^{+5.06}_{-7.9} \text{ km} \cdot \text{sec}^{-1} \cdot \text{Mpc}^{-1} \text{ [0.11 per mille]}. \quad (1)$$

The predicted expansion rate in Eq. (1) roughly agrees, within the percent-level uncertainty of the comparison, with the best present late-universe determination using the relation between redshift and distance for Type Ia supernovae by the SH0ES collaboration (A. G. Riess et al. 2025)

$$H_0(\text{SH0ES}) = 73.18 \text{ }^{+8.8}_{-8.8} \text{ km} \cdot \text{sec}^{-1} \cdot \text{Mpc}^{-1} \text{ [12 per mille]}. \quad (2)$$

Correspondingly, the predicted expansion rate in Eq. (1) differs sharply, by 8.8σ , from the best present Λ CDM prediction using early-universe observations (Planck Collaboration et al. 2019, 2020)

$$H_0(\Lambda\text{CDM}) = 67.9 \text{ }^{+4.0}_{-4.0} \text{ km} \cdot \text{sec}^{-1} \cdot \text{Mpc}^{-1} \text{ [5.9 per mille]}. \quad (3)$$

The straightforward resolution of the Hubble tension is that the late-universe observations are basically correct (on this point, see also D. Scolnic et al. (2025)), as are the Λ CDM predictions for the value of the cosmological constant and for the value of the present energy density of dark matter in the universe, but that the value of the present energy density of baryons is more than double the value predicted by Λ CDM (See Section 3 for the actual values of the corresponding cosmological parameters and for the comparison with Λ CDM).

In a spatially flat universe, the value of the present expansion rate, $H_0 = 100h \text{ km sec}^{-1} \text{ Mpc}^{-1}$, is linked to the values of the cosmological parameters of the cosmological constant, Λ , the dark matter energy density, u_A , the baryon energy density, u_B , and the photon energy density, u_γ , by the simple relation (P. J. E. Peebles 1993, pg. 100)

$$h^2 = \Omega_A h^2 + \Omega_B h^2 + \Omega_\gamma h^2 + \Omega_\Lambda h^2, \quad (4)$$

where the cosmological parameter is $\Omega_X h^2 = (8\pi/3)(Gu_X/c^2)(h/H_0)^2$ for energy density u_X , with $X = A, B, \gamma$, and it is $\Omega_\Lambda h^2 = (c^2\Lambda/3)(h/H_0)^2$ for the cosmological constant Λ . To resolve the Hubble tension, we propose a new cosmology, based on dark matter in the form of fundamental particles known as axions (S. Weinberg 1978; F. Wilczek 1978), that leads to predictions for the values of the cosmological parameters, $\Omega_A h^2$ and $\Omega_B h^2$, which have the same precision as the cosmological parameter for photons, $\Omega_\gamma h^2 = 2.473 (2) \times 10^{-5}$ [0.88 per mille], set by the precision of the best present estimate of the CMB temperature $T_\gamma = 2.7255 (6)$ K [0.22 per mille] (D. J. Fixsen 2009). Together with the first-principles prediction, within this axion cosmology, for the value of $\Omega_\Lambda h^2$, to an astounding precision of 44 parts per million (ppm), the prediction for H_0 given in Eq. (1) is obtained using Eq. (4).

The linchpin of the analysis leading to this straightforward resolution of the Hubble tension is the following remarkable, numerically exact relation for the ratio of the energy density of baryons to the energy density of axions in the present universe (See Section 4 for the derivation)

$$\frac{\Omega_B h^2}{\Omega_A h^2} = \frac{2}{\pi^2} (x_p y_T)^2 = 0.393\ 565\ 531, \quad (5)$$

where the numerically exact constant, $x_p = 2.821\ 439\ 372$ (P. J. E. Peebles 1993, pg. 159), gives the kinetic energy, $\check{E} = x_p k T_\pi$, for the axions on the peak of the black-body distribution at the temperature of the Big Bang, $T_\pi = y_T (\chi_{\text{QCD}})^{1/4} / k$, and the numerically exact constant, $y_T = (5/84)^{1/4} = 0.493\ 938\ 274$, relates this temperature to the topological susceptibility of the quantum chromodynamic (QCD) vacuum, $\chi_{\text{QCD}} = (m_A c^2)^2 f_A^2$ (S. Weinberg 1978; F. Wilczek 1978), given by the axion rest-mass energy, $m_A c^2$, and the axion decay constant, f_A . The value of this ratio within Λ CDM cosmology is roughly half as large (Planck Collaboration et al. 2019, 2020). This sharp difference resolves the Hubble tension, as shown in Eq. (1), and has implications for a wide range of astrophysical phenomena, including the formation of large-scale structure during the cross-over from radiation-domination to matter-domination (See Section 5), the synthesis of the nuclei of the chemical elements with low atomic mass during the Big Bang (See Section 6), and the spectrum of initial fluctuations in energy density at the Big Bang itself (See Section 7).

Yet, the most striking implication, perhaps, is the direct laboratory astrophysics observation of the production of dark matter (See Section 8). As near-infrared light passes through a material that has a static electric polarization within its structural unit cell, such as the common plastic material polystyrene, the magnetic field created by the light, \mathbf{B}_{NIR} , couples to the electric field created by the polarization, \mathbf{E}_{DC} , and their dot product, $\mathbf{E}_{\text{DC}} \cdot \mathbf{B}_{\text{NIR}}$, acts a coherent classical source for axions, provided that the energy of the photons in the light, $h\nu_A$, with the wavenumber, ν_A , matches the rest-mass energy, $m_A c^2$, of the axions. Indeed, a dip in the intensity of near-infrared light transmitted through a thin film of polystyrene was observed (Fig. 1) at roughly

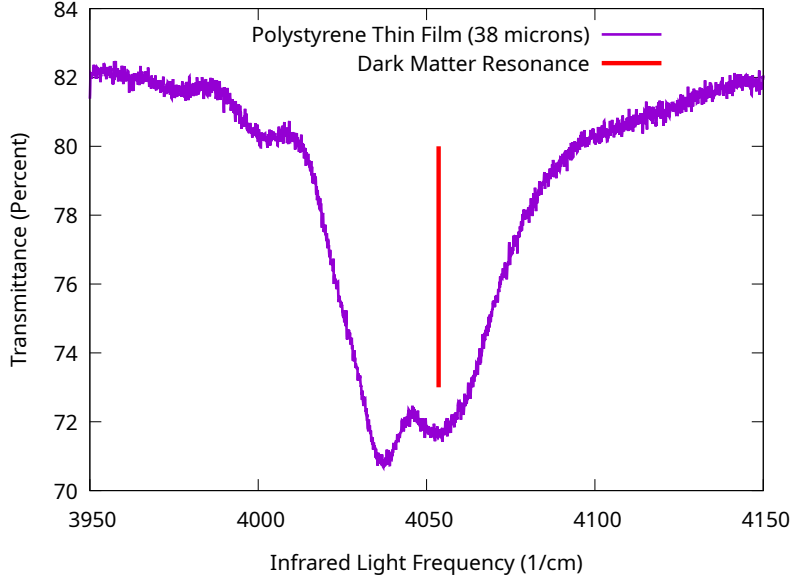


Figure 1. Near-infrared transmittance of polystyrene thin film at room-temperature and ambient pressure with no external static electric or magnetic fields (rough line) shows a decrease when the infrared light frequency is tuned to the resonant value $\nu_A \approx 4054 \text{ cm}^{-1}$ (vertical line, See Eq. (6)), for producing 0.5 eV QCD axion dark matter with the predicted rest-mass energy, $m_A c^2 = h c \nu_A = 0.502 \text{ 580 (2) eV}$ [4.4 ppm].

the predicted wavenumber

$$\nu_A = 4 \text{ 053. 581 (18) cm}^{-1} \text{ [4.4 ppm]}, \quad (6)$$

corresponding to the predicted rest-mass energy of the 0.5 eV QCD axion dark matter,

$$m_A c^2 = 0.502 \text{ 580 (2) eV} \text{ [4.4 ppm]}, \quad (7)$$

and with roughly the size expected from the percent-level precise prediction for the strength of the axion-photon coupling (See Appendix D)

$$g_{A\gamma\gamma} = 0.68 \text{ (2)} \times 10^{-10} \text{ GeV}^{-1} \text{ [3 per cent]}. \quad (8)$$

Finally, a wide range of astrophysical observations have been used over the past five decades to “constrain” or even “exclude” axion dark matter with the rest-mass energy given in Eq. (7) and the axion-photon coupling given in Eq. (8) (See Section 9). Most recently, in 2025, blank-sky observations with the JWST near-infrared spectrometer NIRSpec and mid-infrared spectrometer MIRI (R. Janish & E. Pinetti 2025; S. Roy et al. 2025) were used to derive strong limits on the axion-photon coupling constant, $g_{A\gamma\gamma}$, in the mass range 0.1 to 4 eV, that “exclude,” with much greater than 95% confidence, these predicted values (E. Pinetti 2025). Yet, more than a decade ago, in 2014, observations of horizontal branch stars in globular clusters, combined with stellar evolution that includes the core cooling effects from axion emission due to photon-to-axion conversion in the helium-burning cores of these stars, had already

been used to derive a strong “upper bound” on the value of the axion-photon coupling, $g_{A\gamma\gamma} < 0.66 \times 10^{-10} \text{ GeV}^{-1}$, independent of the value of m_A , which “excludes,” with just over 95% confidence, the predicted value in Eq. (8) (A. Ayala et al. 2014).

In light of the apparent success of 0.5 eV QCD axion dark matter in resolving the Hubble tension, as well as the direct laboratory astrophysical evidence for the predicted axion rest-mass energy and axion-photon coupling, these astrophysical “constraints” and “exclusions” raise important questions about the conventional assumptions for a wide range of astrophysical phenomena. From the velocity dispersion of dark matter in the “halo” of the galaxy to the core helium abundance at formation for stars in globular clusters, these astrophysical assumptions underlie the analyses of the effects of axions on observations and simulations. Turning these analyses on their head, we conclude that the physical picture, presented in this Letter, stimulates a new look at these conventional assumptions, which cut across a wide swath of astrophysical phenomena from star formation to supernovae, from galactic structure to galactic chemical evolution, and from the structure to the evolution of pulsars, white dwarfs, red giants, and horizontal branch stars (See Section 10).

2. 0.5 EV QCD AXION PHYSICAL PICTURE

The physical picture for dark matter, dark energy, and the Big Bang begins with an observation by Y. B. Zel’Dovich (1967). Stimulated by some of the first quasar absorption line spectroscopy (G. Burbidge 1967), a number of astrophysicists suggested a value for the cosmological constant $\Lambda \approx +5 \times 10^{-56} \text{ cm}^{-2}$ (N. Kardashev 1967; J. Shklovsky 1967; V. Petrosian et al. 1967). In this context, Y. B. Zel’Dovich (1967) observed that the gravitational binding energy, U_Λ , generated by a massless particle and antiparticle, each with the kinetic energy, E , separated by the distance, $R = \hbar c/E$,

$$\begin{aligned} U_\Lambda &= N_U G \frac{(E/c^2)^2}{R} \\ &= N_U \frac{E^3}{E_{\text{Pl}}^2}, \end{aligned} \quad (9)$$

with N_U a dimensionless constant of order $\mathcal{O}(10^{-1})$, and having particle-antiparticle pair number density,

$$\begin{aligned} n_\Lambda &= N_n \frac{1}{R^3} \\ &= N_n \left(\frac{E}{\hbar c} \right)^3, \end{aligned} \quad (10)$$

with the dimensionless constant, N_n , of order $\mathcal{O}(10^{-1})$ to prevent Bose-Einstein condensation of the particle-antiparticle pairs, gives cosmological “dark energy” with energy density, $u_\Lambda = U_\Lambda n_\Lambda$, of the right order of magnitude to explain the value of

the cosmological constant, $\Lambda = 8\pi G u_\Lambda / c^4$,

$$\begin{aligned} u_\Lambda &= N_U N_n \left(\frac{E^3}{E_{\text{Pl}}^2} \right) \left(\frac{E}{\hbar c} \right)^3 \\ &= 1.874\,579\,(41) \times 10^{-8} \text{ erg cm}^{-3} [22 \text{ ppm}] \\ &\quad \times \left(\frac{N_U}{0.1} \right) \left(\frac{N_n}{0.1} \right) \left(\frac{E}{105 \text{ MeV}} \right)^6, \end{aligned} \quad (11)$$

provided that the kinetic energy, E , is of the order of $\mathcal{O}(m_p c^2 \times 10^{-1})$, where $m_p c^2 \approx 940 \text{ MeV}$ is the rest-mass energy of the proton and $E_{\text{Pl}} = \sqrt{\hbar c^5 / G} = 1.220\,932\,(13) \times 10^{22} \text{ MeV}$ [11 ppm] is the Planck energy scale:

$$\begin{aligned} E &= (\Omega_\Lambda h^2)^{1/6} \left(\frac{3}{8\pi N_n N_U} \right)^{1/6} (E_{\text{Pl}})^{2/3} \left(\frac{\hbar H_0}{h} \right)^{1/3} \\ &= 86.6\,210\,(6) \text{ MeV} \left(\frac{\Omega_\Lambda h^2}{0.35} \right)^{1/6} \left(\frac{0.1}{N_n} \right)^{1/6} \left(\frac{0.1}{N_U} \right)^{1/6} [7.3 \text{ ppm}]. \end{aligned} \quad (12)$$

In this historical context, the key insight is simply to regard the particle-antiparticle pairs, which are responsible for the dark energy described by the cosmological constant, as forming the dark matter in the universe. The Big Bang, then, is just the moment when massless matter and antimatter bind to form the dark matter, in the form of these particle-antiparticle pairs. As the universe expands, the number density of dark matter, $n_A(t) \propto 1/a(t)^3$, dilutes with the volume of the expanding universe given by the scale factor of the universe, $a(t)$, at time t after the Bang, and, thus, the kinetic energy of the massless matter and antimatter inside the dark matter, $E(t) \propto a(t)$ must grow to keep constant in time the value of the cosmological constant, $\Lambda \propto n_A(t) E(t)^3$.

Starting from the value \check{E} , given by Eq. (12), this kinetic energy reaches its peak value, \hat{E} , at future infinity when the dark matter dissolves and the universe begins contracting. For much of the past four decades, astrophysicists have looked to the Big Bang as a kind of cosmic accelerator for reaching collision energies sufficient to probe phenomena beyond the standard model of particle physics and the standard cold dark matter cosmology (L. Amendola et al. 2018; X. Chen et al. 2017; L. M. Lederman & D. N. Schramm 1989, pg. 161). Yet, it is a simple historical fact that the last generation of the “classic” particle accelerators, known as synchrocyclotrons and built until the 1950s, already reached beam energies sufficient to make pairs of muons (L. M. Lederman & D. N. Schramm 1989, pgs. 93–94), and, thus these classic accelerators already achieved seven decades ago collision energies greater than those typically experienced in the Big Bang, where the typical kinetic energy of radiation, \check{E} , was on the order of, but smaller than, the rest-mass energy of the muon $m_\mu c^2 \approx 106 \text{ MeV}$ (See Eq. (12)).

Instead, the moment in the life-cycle of the universe where the kinetic energy peaks is at future infinity with the value \hat{E} . A natural speculation for this maximum particle

kinetic energy value, $\hat{E} \sim 10^{18}$ MeV, emerges from analysis of the energy dependence of the strengths of the fundamental forces within the standard model of particle physics: It is the energy where these strengths (almost) converge on a “unified” value (L. M. Lederman & D. N. Schramm 1989, pg. 160). But, this appealing (and enduring) speculation then implies that the values for the kinetic energy of the massless particles and antiparticles inside dark matter at the Big Bang, \check{E} , and at future infinity, \hat{E} , satisfy a simple and appealing “see-saw” relation, together with the decay constant, $f_A = \sqrt{\chi_{\text{QCD}}}/(m_A c^2) \sim 10^{10}$ MeV, for the 0.5 eV QCD axion with rest-mass energy, $m_A c^2 \sim 0.5$ eV = 5×10^{-7} MeV (See Eq. (7)):

$$\check{E}\hat{E} = f_A^2, \quad (13)$$

where the best present estimate for the topological susceptibility of the QCD vacuum from Chiral Perturbation Theory (CPT) is $\sqrt{\chi_{\text{QCD}}} = 5690$ (50) MeV² [8.8 per mille] (M. Gorghetto & G. Villadoro 2019).

More rigorously, a per mille precise prediction for the value of the kinetic energy at future infinity, \hat{E} , emerges from simply identifying the value of the axion decay constant, $f_A = \sqrt{\chi_{\text{QCD}}}/(m_A c^2) = 1.132$ (10) $\times 10^{10}$ MeV [8.8 per mille], with the value of the gravitational self-energy created by a pair of massless particles moving with this kinetic energy and separated by the distance, $\hbar c/\hat{E}$:

$$\begin{aligned} f_A &= G \frac{\left(\hat{E}/c^2\right)^2}{\hbar c/\hat{E}} \\ &= \frac{\hat{E}^3}{E_{\text{Pl}}^2}. \end{aligned} \quad (14)$$

Solving Eq. (14), we find the predicted value for the kinetic energy at future infinity with per mille precision:

$$\begin{aligned} \hat{E}(\text{CPT}) &= f_A(\text{CPT})^{1/3} E_{\text{Pl}}^{2/3} \\ &= 1.19\ 05\ (35) \times 10^{18}\ \text{MeV}\ [2.9\ \text{per mille}]. \end{aligned} \quad (15)$$

Indeed, the value $\hat{E}(\text{CPT}) \sim 10^{18}$ MeV is comparable to the “grand unification” energy scale, and, thus, supports the relation given in Eq. (13) between this kinetic energy and that of the Big Bang, \check{E} .

As a consistency check on the basic physical picture, we combine the relations given in Eq. (13) and Eq. (14) to derive a percent-level precise estimate for the value of the kinetic energy at the Bang:

$$\begin{aligned} \check{E}(\text{CPT}) &= f_A(\text{CPT})^{5/3} E_{\text{Pl}}^{-2/3} \\ &= 107.6\ (1.6)\ \text{MeV}\ [15\ \text{per mille}]. \end{aligned} \quad (16)$$

As expected, this value for the kinetic energy at the Big Bang in Eq. (16) is of the same order of magnitude as the estimate based on the value of the cosmological

constant in Eq. (12). To go further, we use in Eq. (12) the actual values of the dimensionless numerically exact constants, $N_U = 1/(2\pi^2) = 0.050\,660\,592$, and, $N_n = 6 \times 2!\zeta(3)/(\pi^2 x_p^3) = 0.065\,072\,004$ (See Appendix A for the derivation of these values from the physical picture):

$$\tilde{E} = 104.218\,7\,(8)\,\text{MeV} \left(\frac{\Omega_\Lambda h^2}{0.35} \right)^{1/6} [7.3\,\text{ppm}], \quad (17)$$

where the still rough but already pleasing agreement between the values in Eq. (16) and Eq. (17) suggests that our physical picture has brought us to the point where we can now estimate the cosmological parameters with confidence from first principles, and, in this way, resolve the Hubble tension.

3. 0.5 EV QCD AXION COSMOLOGICAL PARAMETERS

Within the physical picture sketched in Section 2 (See also Appendix A), the most straightforward cosmological parameter to estimate is that of the 0.5 eV QCD axion dark matter, $\Omega_A h^2$, with the energy density, $u_A = n_A m_A c^2$, given by the axion rest-mass energy, $m_A c^2$, and by the axion number density, n_A :

$$\begin{aligned} n_A &= 6 \times n_\gamma \\ &= 6 \times \frac{2!\zeta(3)}{\pi^2} \left(\frac{kT_\gamma}{\hbar c} \right)^3 \\ &= 2\,464.4\,(1.6)\,\text{cm}^{-3} [0.66\,\text{per mille}], \end{aligned} \quad (18)$$

where the axion-to-photon number ratio, $n_A/n_\gamma = 6$, is set to its value at the Big Bang within the physical picture sketched in Section 2 (For the derivation, see Appendix A). Combining this value for n_A with the value of $m_A c^2$ from Eq. (7), we find a high-precision prediction from first principles for the cosmological parameter of the cold dark matter in the universe,

$$\begin{aligned} \Omega_A h^2 &= \frac{8\pi G}{3c^2} \left(\frac{h}{H_0} \right)^2 m_A c^2 n_A \\ &= 0.117\,542\,(78) [0.66\,\text{per mille}], \end{aligned} \quad (19)$$

where the exact value of the astronomical unit $\text{AU} = 149\,597\,870.700\,\text{km}$ (N. Capitaine et al. 2012) was used to derive the numerically exact value of the cosmological time, $h/H_0 = (\text{AU}/100)(180/\pi)(60)^2 \times 10^6\,\text{sec} = 3.085\,677\,581 \times 10^{17}\,\text{sec}$.

As noted in Section 1, the high-precision prediction from first principles for the cold dark matter cosmological parameter in Eq. (19) agrees to within a percent or so with the best present estimate for this parameter within the standard ΛCDM cosmology using early-universe observations (Planck Collaboration et al. 2019, 2020)

$$\Omega_A h^2(\Lambda\text{CDM}) = 0.118\,82\,(86) [7.2\,\text{per mille}]. \quad (20)$$

Building on this apparent success of our physical picture for dark matter, dark energy, and the Big Bang in bridging the gap between early- and late-universe observations, a quick and dirty estimate of the cosmological constant from first principles is a natural next step. Combining the two estimates of the kinetic energy of radiation at the Big Bang, \check{E} , from Eq. (16) and Eq. (17), and using the high-precision first principles prediction for the value of the present expansion rate from Eq. (1), we get a percent-level precise estimate for the cosmological parameter, Ω_Λ , for the cosmological constant

$$\begin{aligned}\Omega_\Lambda(\text{CPT}) &= (0.35) \left(\frac{107.6 (1.6)}{104.2} \right)^6 \frac{1}{(0.714\ 405)^2} \\ &= 0.831 (75) [90 \text{ per mille}].\end{aligned}\tag{21}$$

Although necessarily rough, the estimate for the cosmological parameter of the cosmological constant in Eq. (21) still agrees to within twenty percent with the best present estimate for this parameter within the standard Λ CDM cosmology using early-universe observations ([Planck Collaboration et al. 2019, 2020](#))

$$\Omega(\Lambda\text{CDM}) = 0.692 (5) [7.2 \text{ per mille}].\tag{22}$$

To push the precision of the first principles estimate of the cosmological constant and to determine the last remaining cosmological parameter, $\Omega_B h^2$, that of the baryons, we must leverage the numerically exact value for the baryon-to-axion energy density ratio, $\Omega_B h^2 / \Omega_A h^2 = 0.393\ 565$, given in Eq. (5), and derived in Sec. 4:

$$\begin{aligned}\Omega_B h^2 &= \Omega_A h^2 \times \left(\frac{\Omega_B h^2}{\Omega_A h^2} \right) \\ &= 0.046\ 260 (31) [0.66 \text{ per mille}],\end{aligned}\tag{23}$$

where the value predicted within our physical picture in Eq. (19) was used for $\Omega_A h^2$. As expected, this high-precision first principles prediction for the baryon abundance in Eq. (23) differs sharply, by more than 180σ , roughly a factor of two, from the best present estimate for this parameter within the standard Λ CDM cosmology using early-universe observations ([Planck Collaboration et al. 2019, 2020](#))

$$\Omega_B h^2(\Lambda\text{CDM}) = 0.022\ 46 (13) [5.8 \text{ per mille}].\tag{24}$$

As discussed in Section 1 (See Eq. (4)), this sharp discrepancy in the value for the baryon abundance predicted with our physical picture and the value predicted with the standard Λ CDM cosmology is the key to resolving the Hubble tension between early- and late-universe observations, since the values of the other cosmological parameters are basically the same in our physical picture as in Λ CDM cosmology.

To attain the promised 44 ppm precision for the value of $\Omega_\Lambda h^2$, it suffices to match the numerically exact baryon-to-axion energy density ratio, given in Eq. (5), with the

value for this ratio computed using straightforward statistical mechanics in thermal equilibrium at the temperature of the Big Bang, $T_\pi = y_T(\chi_{\text{QCD}})^{1/4}/k$, with the numerically exact dimensionless constant $y_T = (5/84)^{1/4} = 0.493\,938\,274$ (See Appendix B for the derivation of y_T):

$$\frac{\Omega_B h^2}{\Omega_A h^2} = \frac{1}{6} \left(\frac{m_p}{m_A} e^{-x_p} I(x_p) + \frac{m_n}{m_A} e^{-x_n} I(x_n) \right), \quad (25)$$

where the axion-to-photon number density ratio, $n_A/n_\gamma = 6$, has been used (See Appendix A for derivation), and the nucleon mass ratio, $x_N = m_N c^2/(kT_\pi)$, for $N = p, n$, determines the equilibrium nucleon-to-photon number density ratio at the Big Bang, $e^{-x_N} I(x_N)$, in terms of the numerically exact integral,

$$I(x_N) = \frac{1}{2!\zeta(3)} \int_0^\infty dx e^{-x} (x + x_N) x^{1/2} (x + 2x_N)^{1/2}. \quad (26)$$

Using the value of the rest-mass of the 0.5 eV QCD axion from Eq. (7), derived in Appendix B, the matching of the baryon-to-axion energy density ratio in Eq. (25) with the numerically exact value predicted in Eq. (5) then determines the temperature of the Big Bang, T_π , to 3.2 ppm, and the topological susceptibility of the QCD vacuum, χ_{QCD} , to 13 ppm:

$$\begin{aligned} kT_\pi &= 36.880\,16 \text{ (12) MeV [3.2 ppm]} \\ \sqrt{\chi_{\text{QCD}}} &= 5\,574.947 \text{ (35) MeV}^2 \text{ [6.3 ppm]}, \end{aligned} \quad (27)$$

where the value of $\sqrt{\chi_{\text{QCD}}}$ agrees with the best present estimate from chiral perturbation theory (CPT) $\sqrt{\chi_{\text{QCD}}}(\text{CPT}) = 5\,690 \text{ (50) MeV}^2$ [8.8 per mille] (M. Gorghetto & G. Villadoro 2019), to within two percent, but is roughly 1400 times more precise. Repeating the quick and dirty calculation of the cosmological constant in Eq. (21), but now with the Big Bang kinetic energy, $\check{E} = x_p kT_\pi = 104.055\,14 \text{ (33) [3.2 ppm]}$, given by the first principles prediction for the Big Bang temperature in Eq. (27), yields the value of the cosmological parameter for the cosmological constant, $\Omega_\Lambda h^2$, to 44 ppm (See Appendix B for the derivation of the precision of the estimate):

$$\begin{aligned} \Omega_\Lambda h^2 &= (0.35) \left(\frac{104.055\,14}{104.218\,7 \text{ (8)}} \right)^6 \\ &= 0.346\,717 \text{ (15) [44 ppm]}. \end{aligned} \quad (28)$$

which combines with the estimates of $\Omega_A h^2$ in Eq. (19) and of $\Omega_B h^2$ in Eq. (23) to give the first-principles prediction for the present expansion rate of the universe in Eq. (1) using Eq. (4), and which agrees within two percent with the Λ CDM value in Eq. (22) for Ω_Λ , given by

$$\begin{aligned} \Omega_\Lambda &= \frac{\Omega_\Lambda h^2}{h^2} \\ &= \frac{0.346\,717}{(0.714\,506 \text{ (79)})^2} \\ &= 0.679\,146 \text{ (75) [0.22 per mille]}, \end{aligned} \quad (29)$$

where Eq. (28) was used for the value of $\Omega_\Lambda h^2$ and Eq. (1) was used for the value of h .

4. 0.5 EV QCD AXION-TO-BARYON ENERGY DENSITY RATIO

To derive the numerically exact value of the baryon-to-axion energy density ratio, $\Omega_B h^2 / \Omega_A h^2 = (2/\pi^2)(x_p y_T)^2 = 0.393\,565\,531$, given in Eq. (5), which is the key to the proposed resolution of the Hubble Tension, presented in Sections 1, 2, and 3, we use the cyclic cosmology matching condition (See Appendix C):

$$\left(\frac{T_\pi}{T_\gamma}\right)^3 \left(\frac{\check{E}}{f_A}\right)^2 \Omega_B h^2 = 4 \left(\frac{\hat{E}}{f_A}\right)^2 \Omega_\Lambda h^2, \quad (30)$$

which gives an independent relationship between the baryon energy density and the cosmological constant. To eliminate the cosmological constant and bring in the axion energy density, we use the expression for the cosmological constant, $\Lambda = 8\pi G u_\Lambda / c^4$, in terms of dark energy density, $u_\Lambda = U_\Lambda n_\Lambda$, with the dark energy of particle-antiparticle pairs at the Big Bang, U_Λ , given in Eq. (9) with \check{E} for the kinetic energy, and with the particle-antiparticle pair density, $n_\Lambda = (T_\pi/T_\gamma)^3 n_A$, set to the axion number density at the Big Bang (See Appendix A),

$$\begin{aligned} \Omega_\Lambda h^2 &= \frac{8\pi G}{3c^2} \left(\frac{h}{H_0}\right)^2 \left(N_U G \frac{(\check{E}/c^2)}{\hbar c/\check{E}}\right) \left(\frac{T_\pi}{T_\gamma}\right)^3 n_A \\ &= \left(\frac{1}{2\pi^2} \frac{\check{E}^3}{E_{\text{Pl}}^2}\right) \left(\frac{T_\pi}{T_\gamma}\right)^3 \left(\frac{\Omega_A h^2}{m_A c^2}\right), \end{aligned} \quad (31)$$

where the axion energy density in the present universe, $u_A = m_A c^2 n_A$, was used in the last line, and the value of the dimensionless constant, $N_U = 1/(2\pi^2)$, is derived in Appendix A. Combining the cyclic cosmology matching condition in Eq. (30) with the expression for the cosmological constant in terms of the dark energy density at the Big Bang in Eq. (31), we derive the remarkable, numerically exact baryon-to-axion ratio for energy density in the present universe given in Eq. (5)

$$\begin{aligned} \frac{\Omega_B h^2}{\Omega_A h^2} &= \left(\frac{(T_\pi/T_\gamma)^3 \Omega_B h^2}{\Omega_\Lambda h^2}\right) \left(\frac{\Omega_\Lambda h^2}{(T_\pi/T_\gamma)^3 \Omega_A h^2}\right) \\ &= \frac{2}{\pi^2} \left(\frac{\check{E}}{m_A c^2}\right) \left(\frac{\hat{E}^2}{E_{\text{Pl}}^2}\right) \\ &= \frac{2}{\pi^2} \left(\frac{\check{E}^2}{m_A c^2 f_A} \frac{f_A}{\check{E}}\right) \left(\frac{f_A}{\hat{E}}\right) \\ &= \frac{2}{\pi^2} \left(\frac{\check{E}}{\sqrt{\chi_{\text{QCD}}}}\right)^2 \left(\frac{f_A^2}{\check{E} \hat{E}}\right) \\ &= \frac{2}{\pi^2} (x_p y_T)^2, \end{aligned} \quad (32)$$

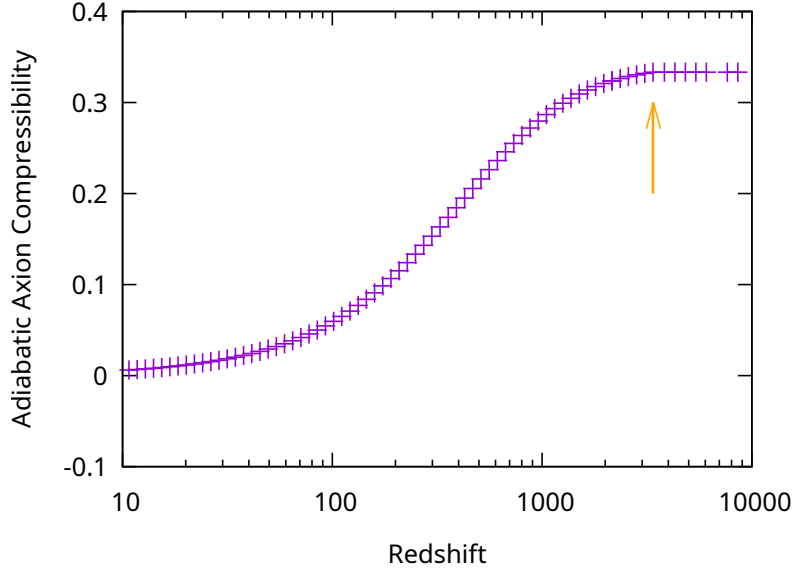


Figure 2. Cooling of 0.5 eV QCD axion dark matter in the early universe shows a cross-over in the adiabatic compressibility, dp_A/du_A (purple crosses), from the radiation-like value, $dp_A/du_A \approx 1/3$, at large redshift, to the matter-like value, $dp_A/du_A \approx 0$, at small redshift, starting right around the redshift of “matter-radiation equality,” $z_{\text{eq}} = 3\,376$ (19) (vertical orange arrow), predicted by the standard cold dark matter cosmology with cosmological constant (Λ CDM) using observations of the early universe (Planck Collaboration et al. 2019, 2020).

where we have used the see-saw relation, $\tilde{E}\hat{E} = f_A^2$, from Eq. (13) in the last line and the dark energy condition at future infinity, $f_A = \hat{E}^3/E_{\text{Pl}}^2$, from Eq. (14) in the third line.

5. 0.5 EV QCD AXION STRUCTURE FORMATION

The formation of large-scale astrophysical structures in the early universe is a key test of any proposal for the nature of dark matter, dark energy, and the Big Bang, including 0.5 eV QCD axion cyclic cosmology. Historically, the now-standard cold dark matter cosmology first emerged in the context of concerns about the relative *lack* of large-scale anisotropy in the cosmic microwave background (CMB), compared to expectations based on the then-standard baryon-based Big Bang cosmology (P. J. E. Peebles 2020, pg. 301–302). In fact, Peebles first proposed a hot dark matter cosmology (P. J. E. Peebles 1982a), before turning to cold dark matter (P. J. E. Peebles 1982b), with the shared goal, in both cases, of “washing out” large-scale CMB anisotropy and, in this way, resolving the tension between the then-standard cosmology and early-universe observations by D. J. Fixsen et al. (1983).

Figure 2 shows the cross-over in the equation of state that relates the pressure, $p_A(z)$, and the energy density, $u_A(z)$, for 0.5 eV QCD axion dark matter in thermal equilibrium with the cosmic background radiation at temperature, $(1+z)T_\gamma$ (P. J. E. Peebles 1993, pgs. 134–135), where z is the redshift and T_γ is the temperature of the CMB. At large redshift, $z \gg 10^4$, the adiabatic axion compressibility,

$dp_A/du_A \approx 1/3$, takes the radiation-like value, reflecting a light-like equation of state, $p_A(z) = u_A(z)/3$ (P. J. E. Peebles 1993, pg. 139), while at small redshift, $z \ll 10^2$, the value crosses over to matter-like, $dp_A/du_A \approx 0$. Crucially, the cross-over begins at roughly the best present estimate of the redshift for “matter-radiation equality,” $z_{\text{eq}} = 3\,376$ (19) (Planck Collaboration et al. 2019, 2020), within the standard cold dark matter cosmology.

As the 0.5 eV QCD axion dark matter equation of state crosses over to matter-like at small redshifts from radiation-like at large redshifts, starting around z_{eq} , as shown in Fig. 2, the dynamics of the expansion change to “matter-dominated” from “radiation-dominated.” Indeed, with six axions for each photon made in the cosmic background radiation (See Section 3 and Appendix A), axions dominate the expansion dynamics on both sides of “matter-radiation equality.” The cross-over in the axion equation of state (Fig. 2), beginning around z_{eq} , drives the cross-over in the character of the expansion which then drives the large-scale formation seen by early-universe observations, just as the change from “radiation-domination” to “matter-domination” drives such structure to form in the standard cold dark matter cosmology (P. J. E. Peebles 1993, pgs. 624–625).

The rough agreement, shown in Fig. 2, between the best present observational value of the redshift where large-scale structure formation begins, z_{eq} , and the predicted value for this redshift based on the cross-over in the equation of state for the 0.5 eV QCD axion dark matter, is a crucial test for the proposed cosmology. Together with the striking agreement between the predicted and observed values for the present energy density of cold dark matter in the universe (See Section 3), this agreement on large-scale structure formation provides compelling evidence that the proposed 0.5 eV QCD axion dark matter cosmology is compatible with early-universe observations. In this way, we deepen the proposed resolution of the Hubble tension, sketched in Section 1, by ensuring that the agreement between the standard Λ CDM cosmology and early-universe observations is not spoiled by the switch to “cooling” dark matter, in the form of 0.5 eV QCD axion dark matter with the equation of state shown in Fig. 2.

6. 0.5 EV QCD AXION NUCLEOSYNTHESIS

As the expanding universe cools in the first three minutes after the Big Bang (Fig. 3), the mix of particles with a light-like equation of state sets the time, t_d , that it takes to “turn off” the photodisintegration of the deuteron, d , so that the nuclei of light chemical elements beyond hydrogen, mainly helium, can form (P. J. E. Peebles 1993, pgs. 184–186). Remarkably, the resulting “primordial” helium abundance (by mass), $Y_{\text{p}} \approx 0.3$, does not depend much on the baryon number density, $n_B(T_d)$, at the “turn-off” temperature, $T_d \approx 10^9$ K (P. J. E. Peebles 2020, pg. 129). Instead, the main constraints on baryon abundance from Big Bang nucleosynthesis (BBN) come from comparisons with observations of the “primordial” deuterium abundance (by

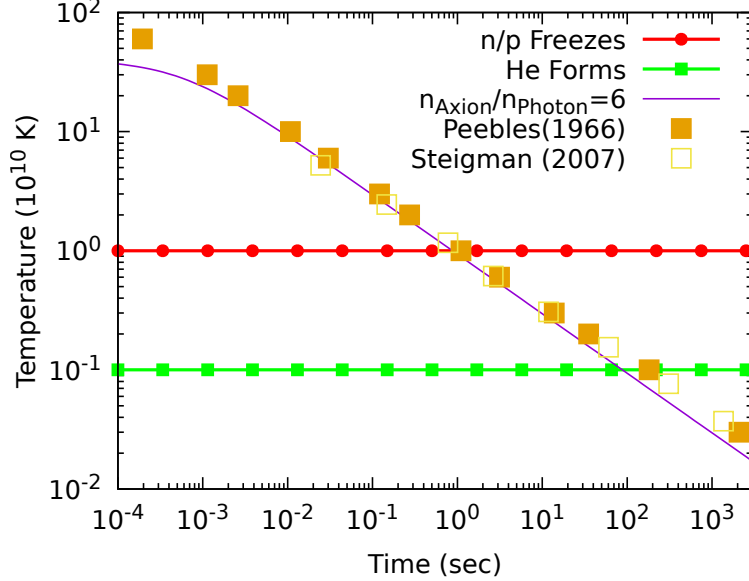


Figure 3. Cooling of the universe in the first three minutes after the Big Bang for a mix with six 0.5 eV QCD axions for each photon (curved line) and for the standard mix of photons and light leptons (filled and unfilled boxes) both reach the freeze-out of the neutron-to-proton ratio (horizontal line with dots) around the same time, but the standard mix (P. J. E. Peebles 1966; G. Steigman 2007) takes roughly twice as long to start forming helium nuclei (horizontal line with boxes).

number), $n_d/n_p = 2.55 (3) \times 10^{-5}$ (R. J. Cooke et al. 2018), based on quasar absorption line spectroscopy.

Indeed, doubling the baryon number density, $n_B(T_d)$, compared to the standard cold dark matter cosmology value, as we propose to do to resolve the Hubble tension (See Section 1 and 3), ensures a nearly complete conversion of deuterons into helium, and, thus, a nearly complete *absence* of primordial deuterium (R. J. Cooke et al. 2018), for the timing of the turn-off, $t_d(\Lambda\text{CDM}) \approx 200$ sec (P. J. E. Peebles 1966; G. Steigman 2007), set by the standard mix of light leptons and photons. Yet, with the appropriate mix of six axions for every photon made in the Big Bang (See Section 3 and Appendix A), the turn-off time, $t_d \approx 100$ sec, comes nearly twice as fast as it does with the standard mix (See Fig. 3). Thus, the value of the product that determines the deuterium abundance, $n_B(T_d)\langle\sigma v\rangle t_d \sim 1$, lands in about the same place, preserving the agreement with observations, where $\langle\sigma v\rangle$ is the thermal average of the product of the neutron capture cross-section, σ , with the nucleon relative velocity, v , (P. J. E. Peebles 1993, pg. 141–142).

Still, the change in the time of the turn-off, t_d , has observable consequences due to the change in the gap in time, $t_d - t_n$, between the start of BBN, at t_d , and the “freeze-out,” at t_n , of the weak nuclear reactions between light leptons and nucleons (Fig. 3). During this gap, the decay of free neutrons with life-time, $\tau_n \approx 878$ sec (P. J. Mohr et al. 2025), cuts down the neutron-to-proton ratio (P. J. E. Peebles 1993, pg. 184–186). By cutting t_d , while leaving t_n more or less unchanged, we shorten the gap,

$t_d - t_n$, by about ten percent of the free neutron lifetime, τ_n , so that about ten percent more neutrons make it to the start of BBN, at t_d , after which essentially all the surviving free neutrons end up as primordial helium (P. J. E. Peebles 2020, pg. 128–129): We thus expect a roughly ten percent larger value for the primordial helium abundance, $Y_P \approx 0.27$, compared to the best present estimate with the standard mix of light leptons and photons, $Y_P(\Lambda\text{CDM}) \approx 0.25$ (C. Pitrou et al. 2018; S. Gariazzo et al. 2022).

7. 0.5 EV QCD AXION INITIAL FLUCTUATIONS

More than five decades ago, E. R. Harrison (1970) and Y. B. Zeldovich (1972) argued for a scale-invariant initial spectrum of fluctuations in the energy density of the radiation created in the Big Bang, $P(k) = Ak^{n_s}$, where the spectral index value, $n_s = 1$, ensures scale-invariance, and the constant, A , is independent of the co-moving wavevector of the fluctuation, k . Within the standard ΛCDM cosmology, the best present estimate from early-universe observations for the value of the spectral index, $n_s(\Lambda\text{CDM}) = 0.9677$ (37) (Planck Collaboration et al. 2019, 2020), falls 8.8σ below the scale-invariant value, $n_s = 1$. By contrast, the conformal symmetry of the cross-over from future infinity to the next big bang in 0.5 eV QCD axion cyclic cosmology (See Appendix C) *requires* the scale-invariant value, $n_s = 1$, in agreement with the argument of E. R. Harrison (1970) and Y. B. Zeldovich (1972), but in sharp tension (8.8σ) with the standard ΛCDM value.

8. 0.5 EV QCD AXION LABORATORY ASTROPHYSICS

Figure 1 shows the laboratory astrophysics evidence for 0.5 eV QCD axion dark matter with the rest-mass energy, $m_A c^2$, predicted in Eq. (7), and the corresponding prediction for the axion-photon coupling strength, $g_{A\gamma\gamma}$, given in Eq. (8) and derived in Appendix D. The data were obtained with a standard commercial infrared spectrometer (Thermo-Fisher Scientific, Nicolet iS50R Fourier Transform Infrared Spectrometer, 0.125 cm^{-1} resolution, KBr beamsplitter, DTGS photodetector at 293 K, Jacquinot stop diameter $w = 1\text{ mm}$), and a polystyrene thin film sample (International Crystal Laboratories, $t = 38\ \mu\text{m}$ thick, 293 K, 1 atm, in air, no external applied electric or magnetic fields, density $\rho = 1.04\text{ g/cm}^3$, unit cell molar mass $\mu = 104\text{ g/mol}$) that is similar to the standard reference material used to calibrate the infrared light frequency response of such spectrometers (NIST 2025). The depth of the dip in transmittance, $\Delta T \approx 0.15 T$, relative to the background transmittance, $T \approx 82\%$, observed at roughly the value of the infrared light frequency predicted for the 0.5 eV QCD axion dark matter resonance, $\nu_A \approx 4054\text{ cm}^{-1}$ (See Eq. (6)), with line-width, $\Delta\nu \approx 30\text{ cm}^{-1}$, has roughly the expected size (F. Wilczek 1978; S. Weinberg 1978):

$$\frac{\Delta T}{T} = \frac{1}{2} (m_A c^2 g_{A\gamma\gamma})^2 (\epsilon_0 E_{\text{DC}}^2) \frac{NV}{hc\Delta\nu} \approx 0.15, \quad (33)$$

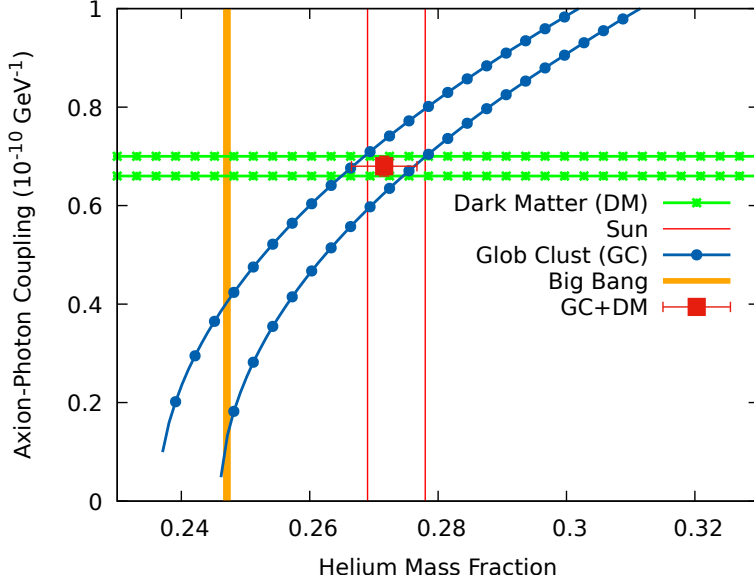


Figure 4. Axion-photon coupling grows with initial core helium mass fraction in simulations of stellar evolution for horizontal branch stars constrained by observations of globular clusters (curved line with dots) (A. Ayala et al. 2014). The predicted value for the axion-photon coupling strength (horizontal lines with boxes), given in Eq. (8), combines with this empirical relation to give a prediction for the helium mass fraction (box with whiskers) that differs by 5.0σ from the primordial helium abundance expected within the standard cold dark matter cosmology with cosmological constant (Λ CDM) based on simulations of Big Bang nucleosynthesis (thick vertical line) (S. Gariazzo et al. 2022; C. Pitrou et al. 2018), but that agrees rather well with the best present estimates for the initial core helium mass fraction in the Sun (pair of thin vertical lines) (L. Piersanti et al. 2007; A. M. Serenelli & S. Basu 2010).

where the static electric field within the unit cell of the plastic has strength $E_{\text{DC}} \approx 5.7 \times 10^8$ V/cm (J. L. Brédas & G. B. Street 1985), the infrared beam within the plastic film has volume $V = (\pi/4)w^2t = 3.0 \times 10^{-5}$ cm³, and the number of unit cells within this volume is $N = N_A \rho V / \mu = 1.8 \times 10^{17}$.

9. 0.5 EV QCD AXION ASTROPHYSICAL CONSTRAINTS

Attempts to “constrain” or “exclude” 0.5 eV QCD axion dark matter using astrophysical phenomena can be grouped by the particle to which the axion couples to create the effect: photon, electron, or nucleon. For axion-photon coupling, the most recent attempts are based on the spontaneous two-photon decay of 0.5 eV QCD axions in the dark matter “halo” of the Milky Way (E. Pinetti 2025; R. Janish & E. Pinetti 2025; S. Roy et al. 2025), while a more established approach looks for axion production from gamma rays in the cores of horizontal branch stars within globular clusters (A. Ayala et al. 2014). Efforts involving axion-electron coupling go back five decades (K. Sato & H. Sato 1975; K. Sato 1978), focused mainly on red giants and white dwarfs, while attempts invoking axion-nucleon coupling have instead looked at pulsars and supernova 1987A (See A. Caputo & G. Raffelt (2024) for a recent review).

Figure 4 shows the empirical relation between the axion-photon coupling strength, $g_{A\gamma\gamma} = g_{10} \times 10^{-10} \text{ GeV}^{-1}$, and the initial core helium mass fraction, Y_{HB} , for stars that are now on the horizontal branch (HB) of the color-magnitude diagram for globular clusters (A. Ayala et al. 2014):

$$R = 6.26Y_{\text{HB}} - 0.41g_{10}^2 - 0.12, \quad (34)$$

where $R = N_{\text{HB}}/N_{\text{RGB}} = 1.39$ (3) was the observed ratio of the number of HB stars, N_{HB} , to the number of stars on the red giant branch (RGB) of the color-magnitude diagram, N_{RGB} , in 39 globular clusters. Combining the empirical relation in Eq. (34) with the predicted value for the axion-photon coupling in Eq. (8), we find a percent-level precise estimate for the initial core helium mass fraction in these HB stars that formed in the first billion years after the Big Bang:

$$Y_{\text{HB}} = 0.272 \text{ (5) [18 per mille]}, \quad (35)$$

which differs by 5σ with the best present estimate of the “primordial” helium abundance, $Y_P(\Lambda\text{CDM}) = 0.24709$ (17) [0.69 per mille] (C. Pitrou et al. 2018; S. Gariazzo et al. 2022), within the standard cold dark matter cosmology, but that roughly matches the best present estimates for the initial core helium mass fraction in the Sun, $Y_{\odot} = 0.273$ (6) [22 per mille] (A. M. Serenelli & S. Basu 2010; L. Piersanti et al. 2007). As discussed in Section 6, the mix of axions and photons that dominates the expansion of the universe leading up to Big Bang nucleosynthesis, within the proposed physical picture, yields about ten percent more primordial helium, $Y_P \approx 0.27$, than the standard mix of light leptons and photons, and, in this way, resolves the 5σ tension between Y_{HB} in Eq. (35) and $Y_P(\Lambda\text{CDM})$.

Similarly, the recent attempts to “rule out” axion dark matter with the rest-mass energy and axion-photon coupling indicated by laboratory astrophysics (See Section 8), using “blank-sky” observations of the dark matter “halo” of the Milky Way at the near-infrared wavelength $2\lambda_A = 2h/m_Ac \approx 4.93 \mu\text{m}$, corresponding to the decay of the axion into a pair of photons, subtract a “smooth astrophysical background” by fitting a quartic polynomial to the near-infrared spectrum within a window of width $\Delta\lambda \approx 0.2 \mu\text{m}$ (E. Pinetti 2025). However, the proposed physical picture implies that 0.5 eV QCD axion dark matter is in thermal equilibrium with the cosmic microwave background (See Section 3 and Appendix A), and, thus, the axions in the dark matter “halo” of the Milky Way have velocity dispersion, σ_v , fixed by the CMB temperature, T_{γ} , and by the 0.5 eV QCD axion dark matter rest-mass energy, m_Ac^2 , leading to an expected line-width, $2\Delta\lambda_A$, that is roughly the same size as the window used to subtract the “smooth astrophysical background:”

$$\begin{aligned} 2\Delta\lambda_A &= 2\lambda_A \frac{\sigma_v}{c} \\ &= 2\lambda_A \sqrt{\frac{3kT_{\gamma}}{m_Ac^2}} \\ &\approx 0.2 \mu\text{m}. \end{aligned} \quad (36)$$

Instead of “constraining” the 0.5 eV QCD axion, the analysis by [E. Pinetti \(2025\)](#) in effect rules out the standard cold dark matter velocity dispersion, $\sigma_v(\Lambda\text{CDM}) \approx 200 \text{ km sec}^{-1}$ ([M. W. Goodman & E. Witten 1985](#)), which is based on the assumption of gravitational equilibrium with “bright” matter, such as OB associations, H II regions, and 21 cm clouds, and that is much smaller than the velocity dispersion, $\sigma_v \approx 11,000 \text{ km sec}^{-1}$, given in Eq. (36) by thermal equilibrium with the CMB, within the proposed physical picture.

Turning to axion-electron coupling, the key point is that there is no “tree-level” or “bare” coupling between the axion and electron [R. D. Peccei \(1989\)](#), just as there is no such coupling between the neutral pion, π^0 , and the electron ([T. Husek 2024](#)). Instead, the “leading order” axion-electron coupling appears only at “loop-level,” and is suppressed by the small factor, $(\frac{\alpha}{2\pi})^2 \sim 10^{-6}$ ([P. J. Mohr et al. 2025](#)), compared to the “bare” value used to derive astrophysical “constraints” and “exclusions” ([K. Sato & H. Sato 1975](#); [K. Sato 1978](#); [A. Caputo & G. Raffelt 2024](#)). The upshot is that the effect of axions on the astrophysical phenomena, such as white dwarf cooling and red giant luminosity, is smaller than the astrophysical uncertainties entering the analysis, and, thus, no significant “constraints” or “exclusions” emerge from the comparison with astrophysical observations.

Finally, regarding the axion-nucleon coupling, a dense bunch of nucleons makes a lot of 0.5 eV QCD axions due to this coupling, but, by the same token, such a dense nuclear soup is “axionically thick,” in the sense that a 0.5 eV QCD axion made by one nucleon is unlikely to “escape” the concentration without coupling to another nearby nucleon, as pointed out by [M. S. Turner \(1988\)](#), in the analysis of the effect of axions on supernova 1987A. Remarkably, there is a relatively narrow window of QCD axion rest-mass energy, $0.05 \text{ eV} \leq m_A c^2 \leq 5 \text{ eV}$ ([W. Yin 2023](#), pg. 42), that brackets the predicted value in Eq. (7), in which the effects of the QCD axions completely dominate the flow of energy within the dense nuclear soup, in sharp contrast with the traditional assumption that axions play essentially no role in this flow, and this contrast is often expressed as an “exclusion” of the 0.5 eV QCD axion. However, given the direct laboratory astrophysics evidence for 0.5 eV QCD axion dark matter, sketched in Section 8, one is instead led, on the basis of this analysis of the axion-nucleon coupling, to question “astrophysicists’ most cherished beliefs” ([A. Burrows et al. 1989](#)) regarding the flow of energy within compact astrophysical bodies, such as pulsars, and within the “core-collapse” supernovae that are thought to form such bodies.

10. CONCLUSIONS

Among astrophysicists during the past forty years, three main “pillars” have come to be viewed as supporting the now-standard cold dark matter cosmology (ΛCDM): the anisotropy of the cosmic microwave background (CMB), the “primordial” abundance of chemical elements with low atomic mass whose nuclei were synthesized in the Big

Bang (BBN), and the redshift-magnitude relation of Type Ia supernovae (P. J. E. Peebles 2020, pg. 323–340). The physical picture of dark matter, dark energy, and the Big Bang, presented in this Letter, rests on the same “pillars” of support, but does so more naturally. In particular, the proposed physical picture naturally resolves the 5.0σ tension in the present expansion rate of the universe between Λ CDM and “late” universe observations, and does so in favor of the observations.

Still, most of the cosmological parameters come out with around the same values as they do in Λ CDM. The energy density of cold dark matter in the present universe and the cosmological constant, for example, land within the uncertainties of the best present Λ CDM values from fits to early universe observations. However, it is crucial to emphasize that these essentially shared values arise as first-principles predictions, not fits to observations, within the proposed physical picture.

Similarly, the redshift of “matter-radiation equality” and the “primordial” deuterium abundance come out about the same as Λ CDM. This redshift is the critical “epoch” in the early universe where large-scale structure begins to form, and its value determines the location of the main “peak” in the angular power spectrum of the CMB fluctuations. Likewise, the primordial deuterium abundance is a key indicator of the timing and the conditions in the Big Bang when “light” element nucleosynthesis begins.

In conclusion, what the standard Λ CDM cosmology does well, the present physical picture does just as well or better. More sharply, the present physical picture provides an actual physical picture for the main ingredients of Λ CDM: dark matter, dark energy, and the Big Bang. In this sense, Λ CDM can be viewed, as it was intended to be viewed (P. J. E. Peebles 1993, pg. 621–622), as a way of stimulating “the development of ideas on how to find and test models for the origin of [large-scale] structure,” rather than as an actual physical picture for the nature of dark matter (or anything else).

Moving forward, the sharp difference in the baryon abundance, roughly 180σ , gives about a factor of two more baryons with the present physical picture. At the same time, the mix of six axions for every photon made in the Big Bang, within this picture, speeds up the cooling off of the universe in the first three minutes. The combination of these two sharp differences leads to about the same deuterium abundance but about 5σ more helium compared to Λ CDM, we have argued, and these loose arguments, in part based on astrophysical observations of globular clusters, must be confirmed by actual BBN calculations within the proposed physical picture.

In a similar vein, an actual calculation of the spectrum of CMB fluctuations within the proposed physical picture must be done. We have argued, indirectly, that the location of the main peak in the spectrum should come out about the same as it does in Λ CDM due to the coincidence of the redshift where the 0.5 eV QCD axion dark matter equation of state crosses over from radiation-like to matter-like, on the one hand, and, on the other, the redshift of “matter-radiation equality” within Λ CDM.

Along similar lines, there is reason to believe that the sharp difference in baryon abundance, roughly 180σ , combines with the sharp difference in the “primordial” spectral index, nearly 9σ , to give basically the same spectrum as the best fit within Λ CDM, so that the agreement of this best fit with early universe observations is retained in the present physical picture, albeit with first-principles predictions taking the place of the key fit parameters.

Finally, and perhaps most importantly, the direct laboratory astrophysics evidence for the creation of 0.5 eV QCD axion dark matter in a straightforward, “table-top” experiment, presented in this Letter, suggests that we must “re-visit” many of the conventional assumptions about the way dark matter interacts with light energy and “bright” matter. For much of the past half century, it has been conventional to assume that dark matter “tracks” bright matter in gravitational equilibrium within a “halo” around the Milky Way galaxy, but the direct laboratory astrophysics evidence for 0.5 eV QCD axion dark matter, when combined with the lack of a sharp two-photon decay “line” from 0.5 eV QCD axion dark matter in the infrared spectrum of this halo, suggests that dark matter is, instead, in thermal equilibrium with the photons of the CMB, as predicted by the proposed physical picture. Even more iconoclastically, the direct laboratory evidence for 0.5 eV QCD axion dark matter, when combined with long-standing analyses of the effects of axion-nucleon coupling on dense nuclear soup in astrophysical settings, suggests that “astrophysicists’ most cherished beliefs” about core-collapse supernovae and the internal structure of pulsars are simply wrong, and that, instead, 0.5 eV QCD axion dark matter completely dominates the flow of energy within compact astrophysical bodies and within the events that form them.

ACKNOWLEDGMENTS

Daria Mazura provided critical and constant support without which the work reported here would not have been possible.

APPENDIX

A. 0.5 EV QCD AXION SELF-ENERGY AND NUMBER DENSITY

Within the physical picture presented in Section 2, the gravitational self-energy of 0.5 eV QCD axion dark matter, $U_\Lambda = N_U G(E/c^2)^2/R$, given in Eq. (9), is generated by the kinetic energy, E , of a massless particle and anti-particle, each with de Broglie wavelength, $\lambda = hc/E = 2\pi R$. The value of the dimensionless constant, $N_U = 1/(2\pi^2)$, then follows from two assumptions. First, the axion is “spin-less,” in the sense that the plane of motion of the particle and anti-particle has equal probability amplitude to be oriented in any direction in three-dimensional space, and, second, the three-dimensional vector, \mathbf{r} , separating the particle and anti-particle, is related to twice the de Broglie wavelength, $D = 2\lambda$, by the familiar geometric relation,

$1/D = \langle 1/|\mathbf{r}| \rangle_\Omega$, for the angle-averaged plane-projected (“line-of-sight”) distance (V. Barger & M. Olsson 1995, pgs. 338–339):

$$\begin{aligned} \frac{1}{D} &= \left\langle \frac{1}{|\mathbf{r}|} \right\rangle_\Omega \\ &= \frac{1}{4\pi} \int \frac{d\Omega}{r \sin \theta} \\ &= \frac{1}{4\pi r} \int_0^\pi d\theta \int_0^{2\pi} d\phi \\ &= \frac{\pi}{2r}, \end{aligned} \tag{A1}$$

where, r is the three-dimensional separation, Ω is the solid angle on the two-dimensional sphere of orientations of the orbital plane of the particle-antiparticle pair relative to some fixed “line-of-sight,” θ is the polar angle (co-altitude) of the line-of-sight to the normal vector of the plane, and ϕ is the azimuthal angle of this normal vector with respect to the line-of-sight.

Using the geometric identity in Eq. (A1), it is then straightforward to derive the gravitational self-energy of the 0.5 eV QCD axion dark matter:

$$\begin{aligned} U_\Lambda &= G \frac{(E/c^2)^2}{r} \\ &= \frac{2}{\pi} G \frac{(E/c^2)^2}{D} \\ &= \frac{1}{2\pi^2} G \frac{(E/c^2)^2}{R}. \end{aligned} \tag{A2}$$

Comparing the last line of Eq. (A2) with the expression for the gravitational self-energy in Eq. (9), we find the value of the dimensionless constant, $N_U = 1/(2\pi^2)$. We emphasize that this result requires that the 0.5 eV QCD axion dark matter be a *spin-less* bound-state of particle and anti-particle, and, thus, the axion must obey Bose-Einstein statistics (L. D. Landau & E. M. Lifshitz 1958, pg. 205), just as photons do (P. J. E. Peebles 1993, pg. 134).

At the Big Bang, the average kinetic energy, $\check{E} = x_p k T_\pi \approx 104$ MeV, given in Eq. (17), is much larger than the 0.5 eV QCD axion dark matter rest-mass energy, $m_A c^2 = 0.5$ eV = 5×10^{-7} MeV, given in Eq. (7). The axion number density at the Big Bang, $n_A(T_\pi)$, is then determined by the Planck distribution function, just as the photon number density at the Big Bang, $n_\gamma(T_\pi)$, is so determined (P. J. E. Peebles 1993, pg. 134–137, 158–159), with the result

$$\begin{aligned} n_A(T_\pi) &= \frac{g_A}{2} \frac{2! \zeta(3)}{\pi^2} \left(\frac{k T_\pi}{\hbar c} \right)^3 \\ &= 6 n_\gamma(T_\pi) \\ &= \left(\frac{T_\pi}{T_\gamma} \right)^3 n_A, \end{aligned} \tag{A3}$$

where n_A is the axion number density in the present universe, T_γ is the temperature of the cosmic microwave background, and the statistical degeneracy factor, $g_A = 12$, counts the twelve “flavors” of quarks and leptons in the standard model of particle physics (L. M. Lederman & D. N. Schramm 1989, pg. 128). Each flavor, M , of quark and lepton binds with an anti-particle of the same flavor and helicity to make the axion, A_M , with this flavor and no spin, such that the axion number density at the Big Bang is given by the expression in Eq. (10), with the value of the dimensionless constant, $N_n = 6 \times 2! \zeta(3) / (\pi^2 x_p^3)$, fixed by the result given above in Eq. (A3).

B. 0.5 EV QCD AXION REST-MASS AND BIG BANG TEMPERATURE

The predicted value for the rest-mass energy, $m_A c^2$, of the 0.5 eV QCD axion dark matter, given in Eq. (7), follows from the analysis of the baryon-to-axion energy density ratio, $\Omega_B h^2 / \Omega_A h^2$, presented at the end of Section 3, once a relation can be found with the temperature of the Big Bang, T_π . Both of the quantities, $m_A c^2$ and kT_π , enter the statistical mechanical expression for this ratio, given in Eq. (25), through their ratios with the nucleon rest-mass energies, $m_N c^2$, for $N = n, p$. Given an independent relation between $m_A c^2$ and kT_π , then, the matching of this expression to the numerically exact value for the ratio, $\Omega_B h^2 / \Omega_A h^2 = 2(x_p y_T)^2 / \pi^2$, given in Eq. (5) and derived in Section 4, determines both quantities with a precision that is limited only by that of this independent relation.

The starting point for finding such an independent relation between $m_A c^2$ and kT_π is the relation between the axion decay constant, f_A , and the kinetic energy, \tilde{E} , of the massless particle and anti-particle within the axion at future infinity, given in Eq. (14), combined with the “see-saw” relation for the value of this kinetic energy, $\tilde{E} = x_p kT_\pi$, at the Big Bang, given in Eq. (13):

$$\begin{aligned} f_A &= \left(\frac{f_A^2}{x_p kT_\pi} \right)^3 (E_{\text{Pl}})^{-2} \\ &= f_A \left(\frac{\sqrt{\chi_{\text{QCD}}}}{m_A c^2} \right)^5 (x_p kT_\pi)^{-3} (E_{\text{Pl}})^{-2} \\ &= f_A \frac{1}{x_p^3 y_T^{10}} (kT_\pi)^7 (m_A c^2)^{-5} (E_{\text{Pl}})^{-2} \end{aligned} \quad (\text{B4})$$

where the topological susceptibility of the QCD vacuum, $\chi_{\text{QCD}} = (m_A c^2 f_A)^2$, gives the temperature of the Big Bang, $kT_\pi = y_T (\chi_{\text{QCD}})^{1/4}$, with the dimensionless constant, $y_T = (5/84)^{1/4}$, to be derived at the end of this appendix. Solving for $m_A c^2$ in Eq. (B4), we find the desired independent relation with kT_π :

$$m_A c^2 = x_p^{-3/5} y_T^{-2} (kT_\pi)^{7/5} (E_{\text{Pl}})^{-2/5}. \quad (\text{B5})$$

The precision of this relation is set by the 22 ppm uncertainty in the best present value for the universal gravitational constant, $G = 6.674\,08\,(15) \times 10^{-8} \text{ g}^{-1} \text{ cm}^3 \text{ s}^{-2}$ (P. J. Mohr et al. 2025), and we find the relative uncertainties, $\Delta X/X = |n_X| \Delta G/G$,

for the predicted values of various quantities, X , in terms of the relative uncertainty of G and the power, n_X , of the dependence, $X \propto G^{n_X}$:

$$\begin{aligned}
\frac{\Delta m_A c^2}{m_A c^2} &= \frac{1}{5} \frac{\Delta G}{G} = 4.4 \text{ ppm} \\
\frac{\Delta k T_\pi}{k T_\pi} &= \frac{1}{7} \frac{\Delta G}{G} = 3.2 \text{ ppm} \\
\frac{\Delta f_A}{f_A} &= \frac{3}{35} \frac{\Delta G}{G} = 1.9 \text{ ppm} \\
\frac{\Delta \chi_{\text{QCD}}}{\chi_{\text{QCD}}} &= \frac{4}{7} \frac{\Delta G}{G} = 13 \text{ ppm} \\
\frac{\Delta \Omega_\Lambda h^2}{\Omega_\Lambda h^2} &= 2 \frac{\Delta G}{G} = 44 \text{ ppm}.
\end{aligned} \tag{B6}$$

Finally, we derive the relation, $kT_\pi = y_T (\chi_{\text{QCD}})^{1/4}$, with $y_T = (5/84)^{1/4}$, between the Big Bang temperature, T_π , and the QCD topological susceptibility, χ_{QCD} . The starting point is simply the identification, on the one hand, of the kinetic energy density of the photons and axions created in the Big Bang, $(6+1)(T_\pi/T_\gamma)^4 (\hbar c)^3 u_\gamma$, where $(\hbar c)^3 u_\gamma = (\pi^2/15)(kT_\gamma)^4$ (P. J. E. Peebles 1993, pg. 137) gives the energy density of the cosmic microwave background in the present universe (See Appendix A for the statistical degeneracy factor, $g_A/2 = 6$, that gives the axion-to-photon energy density ratio at the Big Bang), and, on the other hand, of the potential energy density, $\chi_{\text{QCD}}(\Delta\theta_A/6)^2$ (G. 't Hooft 1976a,b), released by the QCD vacuum when the axion ‘‘angle’’ jumps by the amount, $\Delta\theta_A = \pi$, from the value, $\theta_A = \pi$, before the Big Bang to the value, $\theta_A = 0$, after the Big Bang (R. D. Peccei & H. R. Quinn 1977a,b):

$$7 \frac{\pi^2}{15} (kT_\pi)^4 = \chi_{\text{QCD}} \left(\frac{\pi}{6}\right)^2. \tag{B7}$$

Solving Eq. (B7) for kT_π , we find the desired relation.

C. 0.5 EV QCD AXION CYCLIC COSMOLOGY

The cyclic cosmology matching condition, given in Eq. (30), follows from the conformal symmetry of the universe beyond future infinity and before the next big bang (R. Penrose 2016). Massless quarks and leptons, together with their anti-particles, move with the speed of light in a space-time with neither dark matter nor dark energy (See Section 2). The decrease of their kinetic energy from the value at future infinity, $\hat{E} \approx 10^{18}$ MeV, given roughly by Eq. (15), to the value at the next big bang, $\tilde{E} \approx 10^2$ MeV, given roughly by Eq. (16), can then be interpreted as a simple conformal rescaling of the metric tensor of this ‘‘cross-over’’ space-time, g_{ab} , to the metric tensor of future infinity, $\hat{g}_{ab} = \hat{\ell}^2 g_{ab}$, and to the metric tensor of the Big Bang, $\check{g}_{ab} = \check{\ell}^2 g_{ab}$, with the conformal factors, $\hat{\ell}$ and $\check{\ell}$, given by the relations

$$\hat{\ell} = \frac{\hat{E}}{f_A} \approx 10^8$$

$$\check{\ell} = \frac{\check{E}}{f_A} \approx 10^{-8}, \quad (\text{C8})$$

where the value of the axion decay constant, $f_A \approx 10^{10}$ MeV, given in Section 2, ensures the condition $\hat{\ell}\check{\ell} = 1$, which has been suggested previously on geometric grounds (R. Penrose 2016).

With this conformal interpretation, the cyclic cosmology matching condition, given in Eq. (30), simply expresses the conformal rescaling of the Ricci curvature scalar at the cross-over, R , to its value at future infinity, \hat{R} , and at the Big Bang, \check{R} , given by (R. Penrose & W. Rindler 1986, pg. 123)

$$\hat{R}\hat{\ell}^2 = R = \check{R}\check{\ell}^2. \quad (\text{C9})$$

To make the connection, we use the field equations of general relativity to express the value of the Ricci curvature scalar at future infinity, \hat{R} , in terms of the cosmological constant, Λ , and the value at the Big Bang, \check{R} , in terms of the baryon energy density at the Big Bang (R. Penrose & W. Rindler 1986, pg. 20)

$$\begin{aligned} \hat{R} &= 4\Lambda \\ \check{R} &= \frac{8\pi G}{c^4} \left(\frac{T_\pi}{T_\gamma} \right)^3 u_B, \end{aligned} \quad (\text{C10})$$

where u_B is the energy density of baryons in the present universe, T_π is the Big Bang temperature, and T_γ is the temperature of the cosmic microwave background. Combining Eq. (C8), (C9), and (C10), we arrive at the cyclic cosmology matching condition

$$4\Omega_\Lambda h^2 \left(\frac{\hat{E}}{f_A} \right)^2 = \Omega_B h^2 \left(\frac{T_\pi}{T_\gamma} \right)^3 \left(\frac{\check{E}}{f_A} \right)^2, \quad (\text{C11})$$

where $\Omega_\Lambda h^2 = (\Lambda c^2/3)(h/H_0)^2$ is the cosmological parameter for Λ , and $\Omega_B h^2 = (8\pi G u_B/3c^2)(h/H_0)^2$ is that for u_B .

D. 0.5 EV QCD AXION-PHOTON COUPLING STRENGTH

The strength of the axion-photon coupling, $g_{A\gamma\gamma}$, that enters the Lagrangian density, $\mathcal{L}_{A\gamma} = g_{A\gamma\gamma} \phi_A \mathbf{E} \cdot \mathbf{B}$, for the interaction between the axion field, ϕ_A , and the dot product, $\mathbf{E} \cdot \mathbf{B}$, of the electric field, \mathbf{E} , and the magnetic field, \mathbf{B} , is determined by the decay constant of the axion, f_A , and by the dimensionless constant, $C_{A\gamma} = \mathcal{O}(1)$, whose value is of order one (F. Wilczek 1978; S. Weinberg 1978)

$$\begin{aligned} g_{A\gamma\gamma} &= C_{A\gamma} \frac{\alpha}{2\pi} \frac{1}{f_A} \\ &= 1.047\,007\,(2) \times 10^{-13} \text{ MeV}^{-1} C_{A\gamma} [1.9 \text{ ppm}], \end{aligned} \quad (\text{D12})$$

where $\alpha = e^2/(\hbar c) = 1/(137.035\,999\,18\,(2))$ (P. J. Mohr et al. 2025) [1.5 parts per billion] is the best present estimate for the dimensionless electromagnetic ‘‘fine-structure’’ coupling constant, and where we have used, in the second line, the relation

for the QCD axion decay constant, $f_A = \sqrt{\chi_{\text{QCD}}}/(m_A c^2)$ (S. Weinberg 1978; F. Wilczek 1978), together with the values for the axion rest-mass energy, $m_A c^2$, given in Eq. (7), and the QCD topological susceptibility, χ_{QCD} , given by Eq. (27) (See Appendix B for the estimate of the uncertainty in the value of f_A). To estimate the value of $C_{A\gamma}$, we use its relation with the light-quark mass ratio, $m_u/m_d = 0.485$ (19) (Z. Fodor et al. 2016), and with the electromagnetic-to-strong axial anomaly ratio, $E/N = 8/3$, (R. D. Peccei 1989; M. Gorghetto & G. Villadoro 2019),

$$\begin{aligned} C_{A\gamma} &= \frac{E}{N} - \frac{2}{3} \frac{4m_d + m_u}{m_d + m_u} \\ &= 0.65 \text{ (2) [26 per mille]}, \end{aligned} \tag{D13}$$

where the value of the anomaly ratio is set by the fact that all twelve flavors of “normal” quarks and leptons within the standard model of particle physics transform with the same axial charge, $Q_A = +1$, under the continuous axial $U(1)_A$ phase symmetry, $U_A(\alpha) = \exp(iQ_A\alpha)$, while the opposite axial charge, $Q_A = -1$, holds for “mirror” quarks and leptons which have the same correlation between chirality and helicity as “normal” antimatter (Right-handed mirror matter feels the weak nuclear force but left-handed mirror matter does not feel it; See L. M. Lederman & D. N. Schramm (1989), pg. 121–123): The 0.5 eV QCD axion dark matter, A_M , with a given flavor, M , is the unique quantum state formed by superposing the bound state of mirror matter and normal antimatter with the bound state of normal matter and mirror antimatter, such that the particle and the antiparticle with flavor M inside the bound states have the same helicity and chirality, and such that the resulting quantum state for the axion, and hence the axion field, ϕ_A , has the same discrete space-time symmetry properties as the dot product, $\mathbf{E} \cdot \mathbf{B}$, ensuring that the Lagrangian density, $\mathcal{L}_{A\gamma}$, is invariant under these transformations (charge-conjugation, space-inversion, and time-reversal; See L. M. Lederman & D. N. Schramm (1989), pg. 121–123). Finally, we combine Eq. (D12) and Eq. (D13) to find the value for the axion-photon coupling strength given in Eq. (8).

REFERENCES

- | | |
|---|--|
| <p>Adame, A. G., Aguilar, J., Ahlen, S., et al. 2025, JCAP, 2025, 021, doi: 10.1088/1475-7516/2025/02/021</p> <p>Aiola, S., Calabrese, E., Maurin, L., et al. 2020, JCAP, 2020, 047, doi: 10.1088/1475-7516/2020/12/047</p> <p>Amendola, L., Appleby, S., Avgoustidis, A., et al. 2018, Living Reviews in Relativity, 21, 2, doi: 10.1007/s41114-017-0010-3</p> | <p>Ayala, A., Domínguez, I., Giannotti, M., Mirizzi, A., & Straniero, O. 2014, PhRvL, 113, 191302, doi: 10.1103/PhysRevLett.113.191302</p> <p>Balkenhol, L., Dutcher, D., Spurio Mancini, A., et al. 2023, PhRvD, 108, 023510, doi: 10.1103/PhysRevD.108.023510</p> <p>Barger, V., & Olsson, M. 1995, Classical Mechanics (McGraw-Hill), 2nd edn.</p> |
|---|--|

- Brédas, J. L., & Street, G. B. 1985, *JChPh*, 82, 3284, doi: [10.1063/1.448226](https://doi.org/10.1063/1.448226)
- Burbidge, G. 1967, *ApJ*, 147, 851, doi: [10.1086/149072](https://doi.org/10.1086/149072)
- Burrows, A., Turner, M. S., & Brinkmann, R. P. 1989, *PhRvD*, 39, 1020, doi: [10.1103/PhysRevD.39.1020](https://doi.org/10.1103/PhysRevD.39.1020)
- Capitaine, N., Klioner, S., & McCarthy, D. 2012, in *IAU Joint Discussion, IAU Joint Discussion*, 40
- Caputo, A., & Raffelt, G. 2024, arXiv e-prints, arXiv:2401.13728, doi: [10.48550/arXiv.2401.13728](https://doi.org/10.48550/arXiv.2401.13728)
- Chen, X., Wang, Y., & Xianyu, Z.-Z. 2017, *PhRvL*, 118, 261302, doi: [10.1103/PhysRevLett.118.261302](https://doi.org/10.1103/PhysRevLett.118.261302)
- Cooke, R. J., Pettini, M., & Steidel, C. C. 2018, *ApJ*, 855, 102, doi: [10.3847/1538-4357/aaab53](https://doi.org/10.3847/1538-4357/aaab53)
- Fixsen, D. J. 2009, *ApJ*, 707, 916, doi: [10.1088/0004-637X/707/2/916](https://doi.org/10.1088/0004-637X/707/2/916)
- Fixsen, D. J., Cheng, E. S., & Wilkinson, D. T. 1983, *PhRvL*, 50, 620, doi: [10.1103/PhysRevLett.50.620](https://doi.org/10.1103/PhysRevLett.50.620)
- Fodor, Z., Hoelbling, C., Krieg, S., et al. 2016, *PhRvL*, 117, 082001, doi: [10.1103/PhysRevLett.117.082001](https://doi.org/10.1103/PhysRevLett.117.082001)
- Gariazzo, S., F. de Salas, P., Pisanti, O., & Consiglio, R. 2022, *Computer Physics Communications*, 271, 108205, doi: [10.1016/j.cpc.2021.108205](https://doi.org/10.1016/j.cpc.2021.108205)
- Goodman, M. W., & Witten, E. 1985, *PhRvD*, 31, 3059, doi: [10.1103/PhysRevD.31.3059](https://doi.org/10.1103/PhysRevD.31.3059)
- Gorghetto, M., & Villadoro, G. 2019, *JHEP*, 2019, 33, doi: [10.1007/JHEP03\(2019\)033](https://doi.org/10.1007/JHEP03(2019)033)
- Harrison, E. R. 1970, *PhRvD*, 1, 2726, doi: [10.1103/PhysRevD.1.2726](https://doi.org/10.1103/PhysRevD.1.2726)
- Husek, T. 2024, *PhRvD*, 110, 033004, doi: [10.1103/PhysRevD.110.033004](https://doi.org/10.1103/PhysRevD.110.033004)
- Janish, R., & Pinetti, E. 2025, *PhRvL*, 134, 071002, doi: [10.1103/PhysRevLett.134.071002](https://doi.org/10.1103/PhysRevLett.134.071002)
- Kardashev, N. 1967, *ApJL*, 150, L135, doi: [10.1086/180110](https://doi.org/10.1086/180110)
- Landau, L. D., & Lifshitz, E. M. 1958, *Quantum Mechanics, Non-Relativistic Theory*, English translation from Russian original by J. B. Sykes and J. S. Bell (Pergamon Press)
- Lederman, L. M., & Schramm, D. N. 1989, *From Quarks to the Cosmos: Tools of Discovery* (Scientific American)
- Mohr, P. J., Newell, D. B., Taylor, B. N., & Tiesinga, E. 2025, *Reviews of Modern Physics*, 97, 025002, doi: [10.1103/RevModPhys.97.025002](https://doi.org/10.1103/RevModPhys.97.025002)
- NIST. 2025, Certificate of Analysis: Standard Reference Material 1921b, Infrared Transmission Wavelength/Wavenumber Standard,, <https://www.nist.gov/srm>
- Peccei, R. D. 1989, in *Introduction to CP Violation*, ed. C. Jarlskog, 501–551, doi: [10.1142/9789814503280_0013](https://doi.org/10.1142/9789814503280_0013)
- Peccei, R. D., & Quinn, H. R. 1977a, *PhRvL*, 38, 1440, doi: [10.1103/PhysRevLett.38.1440](https://doi.org/10.1103/PhysRevLett.38.1440)
- Peccei, R. D., & Quinn, H. R. 1977b, *PhRvD*, 16, 1791, doi: [10.1103/PhysRevD.16.1791](https://doi.org/10.1103/PhysRevD.16.1791)
- Peebles, P. J. E. 1966, *ApJ*, 146, 542, doi: [10.1086/148918](https://doi.org/10.1086/148918)
- Peebles, P. J. E. 1982a, *ApJ*, 258, 415, doi: [10.1086/160094](https://doi.org/10.1086/160094)
- Peebles, P. J. E. 1982b, *ApJL*, 263, L1, doi: [10.1086/183911](https://doi.org/10.1086/183911)
- Peebles, P. J. E. 1993, *Principles of Physical Cosmology* (Princeton University Press), doi: [10.1515/9780691206721](https://doi.org/10.1515/9780691206721)
- Peebles, P. J. E. 2020, *Cosmology's Century: An Inside History of our Modern Understanding of the Universe* (Princeton University Press), 334–335, doi: [10.1515/9780691201665](https://doi.org/10.1515/9780691201665)
- Penrose, R. 2016, *Fashion, Faith, and Fantasy in the New Physics of the Universe* (Princeton University Press), 386–387
- Penrose, R., & Rindler, W. 1986, *Spinors and space-time. Volume 2: Spinor and twistor methods in space-time geometry.*

- Petrosian, V., Salpeter, E., & Szekeres, P. 1967, *ApJ*, 147, 1222, doi: [10.1086/149122](https://doi.org/10.1086/149122)
- Piersanti, L., Straniero, O., & Cristallo, S. 2007, *A&A*, 462, 1051, doi: [10.1051/0004-6361:20054505](https://doi.org/10.1051/0004-6361:20054505)
- Pinetti, E. 2025, arXiv e-prints, arXiv:2503.11753, doi: [10.48550/arXiv.2503.11753](https://doi.org/10.48550/arXiv.2503.11753)
- Pitrou, C., Coc, A., Uzan, J.-P., & Vangioni, E. 2018, *PhR*, 754, 1, doi: [10.1016/j.physrep.2018.04.005](https://doi.org/10.1016/j.physrep.2018.04.005)
- Planck Collaboration, Aghanim, N., Akrami, Y., et al. 2019, *Planck* 2018 Results: Cosmological Parameter Tables, Baseline Likelihood Combinations with 68% confidence limits, Combination 2.40
- Planck Collaboration, Aghanim, N., Akrami, Y., et al. 2020, *A&A*, 641, A6, doi: [10.1051/0004-6361/201833910](https://doi.org/10.1051/0004-6361/201833910)
- Poulin, V., Smith, T. L., Karwal, T., & Kamionkowski, M. 2019, *PhRvL*, 122, 221301, doi: [10.1103/PhysRevLett.122.221301](https://doi.org/10.1103/PhysRevLett.122.221301)
- Riess, A. G. 2024, in *The Hubble Constant Tension*, ed. E. Di Valentino & Brout Dillon, 3–6, doi: [10.1007/978-981-99-0177-7_1](https://doi.org/10.1007/978-981-99-0177-7_1)
- Riess, A. G., Yuan, W., Macri, L. M., et al. 2022, *ApJL*, 934, L7, doi: [10.3847/2041-8213/ac5c5b](https://doi.org/10.3847/2041-8213/ac5c5b)
- Riess, A. G., Anand, G. S., Yuan, W., et al. 2024a, *ApJL*, 962, L17, doi: [10.3847/2041-8213/ad1ddd](https://doi.org/10.3847/2041-8213/ad1ddd)
- Riess, A. G., Scolnic, D., Anand, G. S., et al. 2024b, *ApJ*, 977, 120, doi: [10.3847/1538-4357/ad8c21](https://doi.org/10.3847/1538-4357/ad8c21)
- Riess, A. G., Li, S., Anand, G. S., et al. 2025, *ApJL*, 992, L34, doi: [10.3847/2041-8213/ae0ad6](https://doi.org/10.3847/2041-8213/ae0ad6)
- Roy, S., Blanco, C., Dessert, C., Prabhu, A., & Temim, T. 2025, *PhRvL*, 134, 071003, doi: [10.1103/PhysRevLett.134.071003](https://doi.org/10.1103/PhysRevLett.134.071003)
- Sato, K. 1978, *Progress of Theoretical Physics*, 60, 1942, doi: [10.1143/PTP.60.1942](https://doi.org/10.1143/PTP.60.1942)
- Sato, K., & Sato, H. 1975, *Progress of Theoretical Physics*, 54, 1564, doi: [10.1143/PTP.54.1564](https://doi.org/10.1143/PTP.54.1564)
- Scolnic, D., Riess, A. G., Murakami, Y. S., et al. 2025, *ApJL*, 979, L9, doi: [10.3847/2041-8213/ada0bd](https://doi.org/10.3847/2041-8213/ada0bd)
- Serenelli, A. M., & Basu, S. 2010, *ApJ*, 719, 865, doi: [10.1088/0004-637X/719/1/865](https://doi.org/10.1088/0004-637X/719/1/865)
- Shklovsky, J. 1967, *ApJL*, 150, L1, doi: [10.1086/180079](https://doi.org/10.1086/180079)
- Steigman, G. 2007, *Annual Review of Nuclear and Particle Science*, 57, 463, doi: [10.1146/annurev.nucl.56.080805.140437](https://doi.org/10.1146/annurev.nucl.56.080805.140437)
- 't Hooft, G. 1976a, *PhRvL*, 37, 8, doi: [10.1103/PhysRevLett.37.8](https://doi.org/10.1103/PhysRevLett.37.8)
- 't Hooft, G. 1976b, *PhRvD*, 14, 3432, doi: [10.1103/PhysRevD.14.3432](https://doi.org/10.1103/PhysRevD.14.3432)
- Turner, M. S. 1988, *PhRvL*, 60, 1797, doi: [10.1103/PhysRevLett.60.1797](https://doi.org/10.1103/PhysRevLett.60.1797)
- Weinberg, S. 1978, *PhRvL*, 40, 223, doi: [10.1103/PhysRevLett.40.223](https://doi.org/10.1103/PhysRevLett.40.223)
- Wilczek, F. 1978, *PhRvL*, 40, 279, doi: [10.1103/PhysRevLett.40.279](https://doi.org/10.1103/PhysRevLett.40.279)
- Yin, W. 2023, *eV Axion Dark Matter*, <https://texasinshanghai.org/>
- Zel'Dovich, Y. B. 1967, *Soviet Journal of Experimental and Theoretical Physics Letters*, 6, 316
- Zeldovich, Y. B. 1972, *MNRAS*, 160, 1P, doi: [10.1093/mnras/160.1.1P](https://doi.org/10.1093/mnras/160.1.1P)